Enhancing etch resistance of hydrogen silsesquioxane via postdevelop electron curing*

Joel K. W. Yang,[a] Vikas Anant, and Karl K. Berggren
Research Laboratory of Electronics, Massachusetts Institute of Technology, Cambridge, Massachusetts 02139

(Received 6 February 2006; accepted 16 October 2006; published 4 December 2006)

In this work, the authors enhanced the etch resistance of the negative-tone electron resist, hydrogen silsesquioxane (HSQ) to CF_4 reactive ion etching (RIE) by curing HSQ after development. They fabricated superconducting nanowires that were 15 nm wide by pattern transfer into a 6-nm-thick layer of NbN using cured HSQ as the etch mask. HSQ was cured using a postdevelop electron-beam exposure step prior to RIE in CF_4 chemistry. This curing step was shown not to impact the resolution of the HSQ structures while increasing their etch resistance. The results of the authors demonstrate that the etch resistance of HSQ can be tuned after development, which is a desirable resist property of HSQ in addition to its high resolution and low line-edge roughness. © *2006 American Vacuum Society.* [DOI: 10.1116/1.2395949]

I. INTRODUCTION

Resist must serve two functions: it must faithfully reproduce a lithographic pattern and then provide resistance to a subsequent etching process. This multiple objective constrains the performance of the resist in each case. For example, resist that is thinly applied provides excellent electron-beam pattern resolution, but at the expense of reduced etch resistance.

Typically, this trade-off can be resolved by using multiple resist layers (e.g., a bilayer or trilayer process) where only the top layer is used as an imaging layer while the bottom layers are used as pattern-transfer layers (see, for example, Refs. 1 and 2). But this approach adds substantial complexity to the process. A simpler approach is to thermally cure the resist after development to enhance its etch resistance.[3] But thermal curing can damage sensitive underlying materials (such as thin superconducting films). Here we demonstrate an electron-bombardment-based curing process for hydrogen silsesquioxane (HSQ) negative-tone electron resist[4] that substantially improves its etch resistance in fluorine-based reactive ion etching (RIE) while preserving patterning resolution and underlying device-material quality.

We demonstrate that 15-nm-wide, 6-nm-thick superconducting niobium nitride (NbN) nanowires can be fabricated by doing a postdevelop electron cure of HSQ before RIE. The following methods were used in our experiments: (1) the first electron-beam exposure was used to define nanowires at 30 kV acceleration voltage using moderate-to-low electron doses, (2) this exposure was followed by resist develop in aqueous tetramethyl ammonium hydroxide (TMAH), and (3) the nanostructures were then reexposed at a much higher dose (e.g., 50 mC/cm^2) before RIE to cure and toughen the resist. We achieved a 40% decrease in HSQ etch rate by exposing the resist to doses as high as 100 mC/cm^2. In addition, we quantified an observed resist shrinkage that accompanied the enhanced etch resistance. Finally, we explained the mechanism of increased etch resistance and shrinkage based on Fourier transform infrared (FTIR) spectroscopy analysis of HSQ films exposed to different doses.

There are many advantages of increasing etch resistance of the resist other than enabling low-temperature processing. First, increasing etch resistance enables a thinner resist layer which can be used to fabricate much narrower nanowires because of the reduced widths of the forward scattering distribution of electrons.[5] Another advantage of using an etch-resistant, thinner resist is that it circumvents structural collapse that occurs in high aspect-ratio structures.[6] In our case, for example, the etch selectivity between noncured HSQ and NbN was ~7:1, with every nanometer of NbN requiring 7 nm of HSQ etch mask. Therefore, to etch through 6 nm of NbN, one would need at least 50 nm of resist, resulting in an aspect ratio >3 for a 15-nm-wide nanowire, which would typically collapse during sample drying.

We have used 70-nm-thick HSQ in the past to fabricate 90-nm-wide NbN wires for making superconducting single-photon detectors[7] by pattern transfer into a thin film of NbN on sapphire substrates. Using HSQ was convenient as we could directly pattern the etch mask. Furthermore, HSQ does not require high-temperature processing which we have observed can result in material damage. For example, preexposure bakes could be performed <90 °C and still yield excellent results.[8]

We inadvertently discovered the usefulness of postdevelop electron-beam exposure of HSQ when we first tried to make narrower (~25-nm-wide) wires using the process described in Ref. 7 and noticed that the only nanowires that were superconducting were those that had been inspected in a scanning-electron microscope (SEM) prior to RIE. In this work, we found that cured HSQ nanostructures were better etch masks, enabling successful pattern transfer into NbN to form continuous 5-μm-long NbN nanowires. In contrast,

*No proof corrections received from author prior to publication.
[a]Electronic mail: ykwjoel@mit.edu

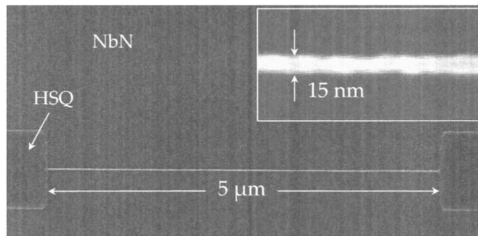

FIG. 1. Scanning electron micrograph (SEM) of a 5-μm-long HSQ nanowire on NbN prior to RIE. The large 1-μm-wide structures at the ends of the wire bridge the nanowire to gold contact pads for electrical measurements. The inset shows a close up of a representative section of the nanowire with a width of 15 nm.

noncured HSQ nanostructures, which were the control samples, were poor etch masks when the starting resist thickness was less than 50 nm.

II. EXPERIMENT

HSQ in the FOx-14 formulation from Dow Corning was diluted in methyl isobutyl ketone (MIBK) in a 1:2 (FOx-14: MIBK) ratio and spin coated onto NbN on sapphire substrates to a thickness of 50 nm. Samples were baked at 90 °C on a hot plate for 5 min to drive out excess solvents. We used a Raith 150 electron-beam lithography (EBL) tool to define nanowire structures by exposing single-pixel lines in the resist at 30 kV using line doses of 1.5–3 nC/cm and at a beam current of 0.3 nA. Samples were then developed in a Microposit® MF CD-26 developer (2.38 wt % aqueous TMAH) for 8 min, rinsed in de-ionized water, and blown dry. Half of the total number of resulting HSQ nanowire structures on one common substrate was then reexposed by exposing 1-μm-wide rectangles aligned to the nanowires in the Raith 150 EBL tool at 30 kV with a beam current of 4 nA and a dose of 50 mC/cm^2 to cure the resist. The other half of the nanowire structures was left uncured and served as control samples. The samples were then etched for 2 min in a Plasmatherm RIE with a CF_4 flow rate of 15 SCCM (SCCM denotes cubic centimeter per minute at STP), chamber pressure was kept at 15 mTorr pressure, and rf power at 100 W. Having cured and noncured HSQ structures on the same substrate ensured identical processing conditions.

To quantify the effects of the electron curing step, we measured the height of the resultant nanowire structures using an atomic force microscope (AFM) before and after RIE for cured as well as noncured HSQ. The same process was repeated to fabricate nanowires on a Si substrate that enabled us to cleave through the nanowires for cross-sectional SEM inspection and measurements using the Raith 150. Care was taken to conduct all processing within 3 days to avoid resist aging.[9]

We measured the dimensions of HSQ nanopillar structures before and after the curing step using the Raith 150 in order to study the effect of curing on resist deformation and resolution. Nanopillar HSQ structures were fabricated on the same Si wafers as the nanowires using single-pixel dots with a dose of 10 fC/dot at a beam current of 0.14 nA.

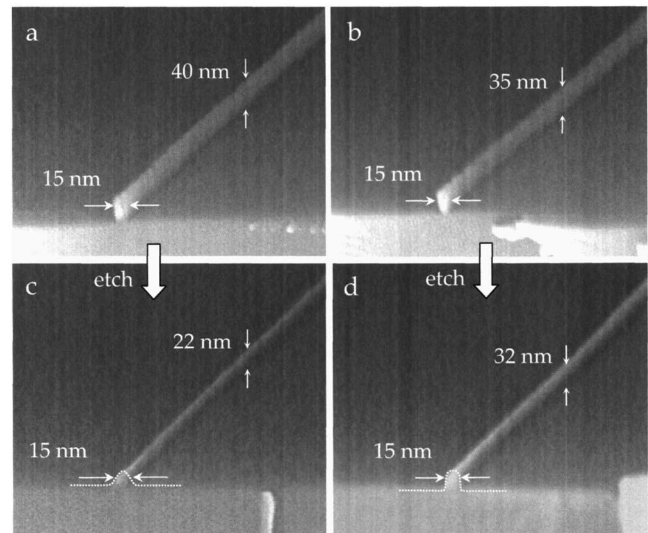

FIG. 2. Scanning electron micrographs (SEMs) of nanowires before [(a) and (b)] and after [(c) and (d)] RIE. For ease of cleaving, the nanowires were fabricated on a Si substrate. (a) SEM of the resultant control (noncured) HSQ structure after exposure and development. (b) SEM of electron-beam cured HSQ structure. We observed a decrease in nanowire height by ~5 nm on average after curing. (c) SEM of the resultant structure after RIE of the control sample. (d) SEM of the resultant structure after RIE using cured HSQ as mask. The dotted lines show a sloped sidewall in control sample and a more vertical sidewall in cured sample. Less material remained after etching the control sample compared to the cured sample.

III. RESULTS AND DISCUSSION

The resultant HSQ nanowires after development range from 15 to 30 nm wide corresponding to line exposure doses from 2.5 to 3 nC/cm. Figure 1 shows a top view of a 15-nm-wide, 5-μm-long HSQ nanowire after development exposed using a dose of 2.5 nC/cm. We saw that nanowires written at lower doses collapsed due to the higher aspect ratio and presumably capillary forces during sample drying. Figure 2(a) shows a cross section of the HSQ nanowire fabricated on a Si substrate. SEM measurements of the HSQ cross section showed that the nanowire structures had an average height of ~45 nm.

Figure 2(b) shows a cured HSQ nanowire structure. Curing the HSQ nanowires caused resist height reduction by 12.5% or 5 nm. There was no noticeable change in wire width for 15-nm-wide wires. In a separate experiment, we saw a decrease in both height and width of 50-nm-wide HSQ structures by as much as 12% after curing with the same conditions as above. We interpreted this consistent fractional reduction in dimension as a result of curing-induced volume shrinkage.

The resultant structures after RIE are shown in the bottom half of Fig. 2 Noncured HSQ was used as the etch mask in Fig. 2(c), while cured HSQ was used as the etch mask in Fig. 2(d). A careful comparison between the two figures revealed that the height of the nanowire was less in Fig. 2(c) than in Fig. 2(d) and the sidewall profile was sloped in Fig. 2(c) but vertical in Fig. 2(d). These observations qualitatively indicate that cured HSQ was a better etch mask than noncured HSQ.

TABLE I. Comparison of resist heights before and after RIE for cured and control (noncured) HSQ nanowires.

	Height before RIE (nm)		Height after RIE (nm)		Etch rate (nm/mm)	
Measurement type	Control	Cured	Control	Cured	Control	Cured
AFM (HSQ on NbN)	45	30	0	12	22.5	9
SEM (HSQ on Si)	40	35	0	12	20	11.5

Quantitatively, as shown in Table I, the etch rate of cured HSQ was lower than that of noncured HSQ. Etch rate calculations required measuring the height of the HSQ structure before etch ($d1$), the height of the nanowire structure after etch ($d2$), and the thickness by which the substrate was etched ($d3$). The measurements of $d1$ and $d2$ were done in the SEM and labeled accordingly as shown in Fig. 2. To determine $d3$, a control Si substrate coated with patterned photoresist as the etch mask was etched alongside the nanowire samples. We then removed the photoresist and measured the etch depth using AFM to obtain $d3$. In this experiment, $d3=10$ nm. Etch rate was then calculated using the expression, $(d1-d2+d3)$/etch time. The thickness of the remaining HSQ in Table I is $d2-d3$.

We also performed AFM measurements of HSQ nanowire thickness for actual superconducting NbN nanowires fabricated on sapphire. As sapphire does not form volatile compounds when etched in CF_4, the measured nanowire height after etching was equal to the thickness of the remaining HSQ plus 6 nm of NbN. We could not do cross-section SEM measurements of the actual nanowires because of the difficulties inherent in cleaving sapphire. Instead we compared AFM measurements of the nanowires to cross-section SEM measurements when the same HSQ nanowire structures were fabricated on Si (discussed above), which enabled easier substrate cleaving. The measurement results are summarized in Table I. There was no remaining noncured HSQ after 2 min of RIE; i.e., the supposedly masked materials (i.e., NbN or Si) were being removed even before etching was complete. AFM measurements also show the same sidewall profiles as observed in the SEM images in Figs. 2(c) and 2(d). NbN is a difficult material to etch (with an etch rate of ~ 3 nm/min in our case) and required 2 min of etching time to pattern transfer into 6 nm of film. The etch selectivity of noncured HSQ to NbN was 7:1 which was poor. Curing HSQ increased the selectivity to 4:1, which represents a substantial improvement over the noncured case.

The results of single-pixel dot exposures were HSQ nanopillars, as shown in Fig. 3. These nanopillars were 50 nm tall with a diameter of 20 nm. We observed nanopillar collapse for structures that had diameters less than 15 nm. The curing step did not cause any undesirable effect on feature shape and size at this length scale as can be seen by comparing Figs. 3(a) and 3(b). This result demonstrates that the etch resistance of HSQ can be increased while preserving structure quality, thus allowing one to simultaneously achieve high resolution and good etching properties.

IV. BULK HSQ ETCH RATE MEASUREMENT EXPERIMENT AND RESULTS

To quantify the effect of resist curing on the etch rate of HSQ, we measured the etch rate dependence on electron dose. These measurements were performed using large structures and allowed us to observe that the increase in etch resistance was due to a modification in the bulk characteristic of HSQ. In this experiment, HSQ was spin coated onto Si substrates to a thickness of 115 nm and baked at 90 °C for 5 min. Rectangles with dimensions of 10 μm wide and 80 μm long were exposed at different electron doses ranging from 100 $\mu C/cm^2$ to 100 mC/cm^2 (equivalent to 6.25–6250 electrons/nm^2) at 30 kV acceleration voltage in the Raith 150 EBL system.

We measured resist shrinkage due to electron bombardment by measuring the difference in resist thickness at the exposed rectangular regions relative to the unexposed surrounding using an AFM scan of the surface. The sample was then developed in Microposit® MF CD-26 for 1.5 min to remove unexposed resist. The remaining resist thickness of rectangles exposed at different doses was again measured using AFM.

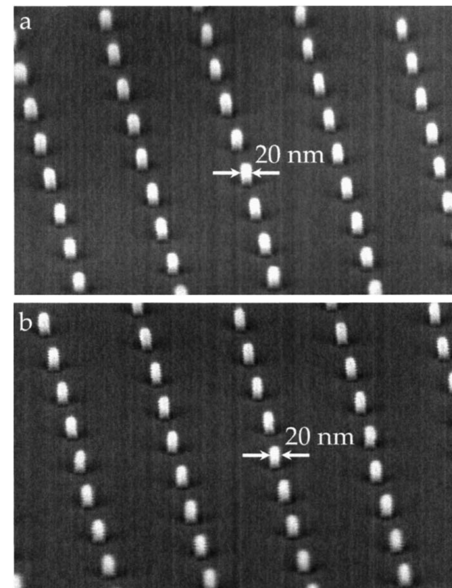

FIG. 3. Scanning electron micrograph (SEM) of HSQ posts (a) before and (b) after curing. Posts were 20 nm wide, 50 nm tall, and arranged in a hexagonal lattice. Reexposing the posts with a dose of 50 mC/cm^2 had no impact on the resulting feature dimensions and shape.

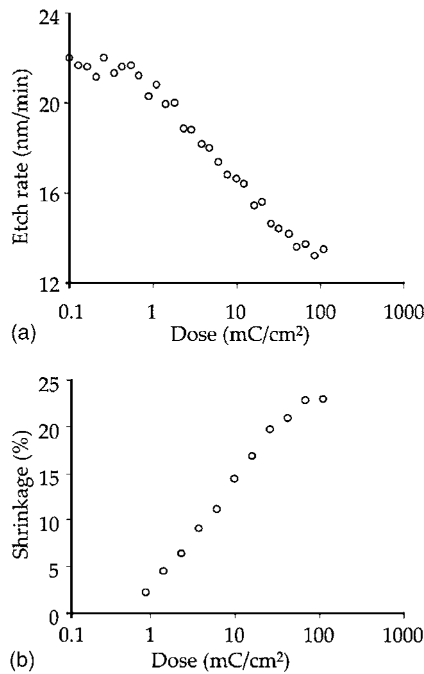

FIG. 4. Plot of HSQ etch rate (a) and shrinkage (b) with respect to electron dose. The etch rate was seen to decrease by 40% after curing the resist using electron doses of 100 mC/cm^2. Maximum amount of shrinkage of 23% occurred with doses greater than 70 mC/cm^2.

We then etched the sample using the same etching conditions as described in Sec. III. In addition, a control Si substrate with a photoresist etch mask was also etched together with the sample. Etch rates were calculated using the same method as explained earlier for calculating etch rates of HSQ nanowires on Si. The etch rate of HSQ was plotted as a function of electron dose in Fig. 4(a). A significant decrease in etch rate by as much as 40% could be observed by comparing etch rates of HSQ exposed at 100 $\mu C/cm^2$ to that exposed at 100 mC/cm^2. These data support the observation in Sec. III that the etch resistance of HSQ can be increased substantially by performing a reexposure step using high electron doses in the range of 50–100 mC/cm^2.

AFM measurements of resist profile after exposure show non-negligible resist shrinkage as plotted in Fig. 4(b). The amount of shrinkage appears to saturate above ~70 mC/cm^2 which could be interpreted as the dose required for complete resist curing. It is important to note that the shrinkage does not totally account for the increased etch resistance. If the increased etch resistance was due only to resist densification, then we would expect the etch rate to decrease by the same amount as the thickness. This was not true as can be seen at the highest curing doses where the resist shrinkage was only ~23% while the etch rate was reduced by ~40%.

FTIR measurements of HSQ exposed to different electron doses are shown in Fig. 5. HSQ was spun onto ZnSe FTIR windows to a thickness of 300 nm and baked at 90 °C for 5 min to drive out excess solvents. 300-μm-diameter disks were exposed at doses of 300 and 2000 $\mu C/cm^2$. The FTIR spectra of the circular areas exposed at different doses were measured using a Spectra Tech Nic Plan FTIR microscope.

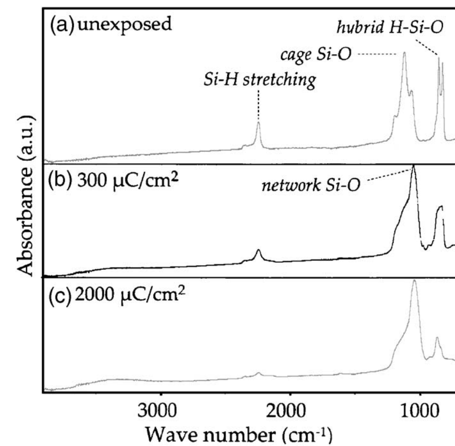

FIG. 5. FTIR spectra of HSQ films that were unexposed (a) and exposed to doses of 300 (b) and 2000 $\mu C/cm^2$ (c). Electron-beam exposure causes Si–H bond scission as well as a shift from cage to network structures. Films exposed to 2000 $\mu C/cm^2$ electron dose had significantly less Si–H bonds compared to films exposed to only 300 $\mu C/cm^2$.

The main absorption peaks of the spectra were identified as Si–H stretching ($2255\ cm^{-1}$), cagelike Si–O stretching ($1120\ cm^{-1}$), and networklike Si–O bonds ($1060\ cm^{-1}$), and peaks in between 800 and 900 cm^{-1} are due to hybrid H–Si–O bond vibrations.[4,10–12]

Si–H bond absorbance peak that decreased in intensity with increasing exposure dose can be taken as a measure of the degree of cross-linking/curing. At high doses, the FTIR spectra become similar to that of SiO_2 (see Ref. 13 and example of SiO_2 spectra). Furthermore, not that the typical exposures used to define structures in EBL (i.e., from 300 to 500 $\mu C/cm^2$) do not completely cross-link HSQ into a SiO_2-like structure. As SiO_2 has a lower etch rate than noncured HSQ in CF_4,[14] the additional curing step before etching is necessary to improve the etch resistance of EBL defined nanostructures by converting HSQ into SiO_2.

The similarity between the FTIR spectra of electron-cured and thermally cured HSQ (Ref. 10) suggests that electron curing achieved the same result as thermal curing. However, thermal curing typically requires baking at temperatures of up to 800 °C for an hour.[15] Such severe processing conditions are damaging for thin superconducting films. Therefore, electron curing is an alternative approach that enables low-temperature processing of devices.

The increased etch resistance of cured HSQ can be understood by comparing its bond strengths and structure density to those of noncured HSQ. As alluded to in Ref. 13, noncured HSQ would have a higher etch rate than SiO_2, and similarly cured HSQ, due to the ease of Si–H bond dissociation in comparison to stronger Si–O network bonds in SiO_2. Moreover, the porosity of the cagelike structure in noncured HSQ makes it easier for fluorine ions to tetrahedrally surround Si atoms on the resist surface and to form volatile SiF_4. Curing therefore increases etch resistance by reducing the amount of cagelike structures and Si–H bonds in HSQ and converting it into SiO_2. The curing-induced shrinkage could be explained as the conversion of porous cagelike mo-

lecular structure into denser network structure typically accompanied by an increase in dielectric constant.[16] Finally, we note that the presence of a broad peak centered around 3400 cm^{-1} in Fig. 5, characteristic of adsorbed water on the film surface,[17] could be due to the hydrophilic nature of cured HSQ. This peak was not present in hydrophobic noncured HSQ.

V. CONCLUSION

We increased the etch resistance of HSQ by performing postdevelop electron-beam curing. We fabricated 15-nm-wide superconducting nanowires using this technique. Electron curing enhanced etch resistance by ~40% and caused resist shrinkage by ~23%. The shrinkage and increased etch resistance were accompanied by an increase in the density of network-Si–O bonds and a simultaneous decrease in Si–H and cage-–Si–O bond densities. This process afforded many advantages, which include direct patterning of etch mask, low-temperature processing (<90 °C), and the avoidance of high aspect-ratio structures which would otherwise collapse. We expect to see this improved performance not just in CF_4 RIE but also in other chemistries.

ACKNOWLEDGMENTS

The authors acknowledge Henry I. Smith, James M. Daley, Mark K. Mondol, and Tim McClure for helpful discussions and technical assistance. The authors also thank G. Gol'tsman and B. Voronov for supplying the NbN films. This work made use of MIT's shared scanning-electron-beam-lithography facility in the Research Laboratory of Electronics. This work is sponsored by AFOSR.

[1] F. C. M. J. M. van Delft *et al.*, J. Vac. Sci. Technol. B **18**, 3419 (2000).
[2] T. A. Savas *et al.*, J. Vac. Sci. Technol. B **14**, 4167 (1996).
[3] L. O'Faolain *et al.*, J. Vac. Sci. Technol. B **24**, 336 (2006).
[4] H. Namatsu *et al.*, Microelectron. Eng. **42**, 331 (1998).
[5] J. J. Hren *et al.*, *Introduction to Analytical Electron Microscopy* (Plenum, New York, 1979).
[6] H. Namatsu, J. Vac. Sci. Technol. B **19**, 2709 (2001).
[7] J. K. W. Yang *et al.*, IEEE Trans. Appl. Supercond. **15**, 626 (2005).
[8] W. Henschel, Y. M. Georgiev, and H. Kurz, J. Vac. Sci. Technol. B **21**, 2018 (2003).
[9] F. C. M. J. M. van Delft, J. Vac. Sci. Technol. B **20**, 2932 (2002).
[10] T. Nakamura *et al.*, Jpn. J. Appl. Phys., Part 1 **40**, 6187 (2001).
[11] J. H. Zhao *et al.*, Appl. Phys. Lett. **74**, 944 (1999).
[12] A. Grill and D. A. Neumayer, J. Appl. Phys. **94**, 6697 (2003).
[13] S. W. Hwang *et al.*, Jpn. J. Appl. Phys., Part 1 **41**, 5782 (2002).
[14] T. E. F. M. Standaert *et al.*, J. Vac. Sci. Technol. A **17**, 741 (1999).
[15] H. C. Liou and J. Pretzer, Thin Solid Films **335**, 186 (1998).
[16] P. T. Liu *et al.*, Thin Solid Films **332**, 345 (1998).
[17] P. T. Liu *et al.*, Electrochem. Solid-State Lett. **5**, G11 (2002).